World Journal of Advanced Research and Reviews
eISSN: 2581-9615 CODEN (USA): WJARAI
Cross Ref DOI: 10.30574/wjarr
Journal homepage: https://wjarr.com/

(RESEARCH ARTICLE)

Check for updates

Valorization of agro-industrial waste into nanoparticle-modified biochar for sustainable wastewater treatment

Sakshi Puranik [1,*], Parimeeta Chanchani [2] and Preeti Pradhan [2]

[1] *Department of Chemistry, Mansarovar Global University, Bilkisganj, Sehore, Madhya Pradesh, India.*
[2] *Department of ESH, Indore Institute of Science and Technology, Indore, Madhya Pradesh, India.*

World Journal of Advanced Research and Reviews, 2026, 31(01), 691–699

Publication history: Received on 30 May 2026; revised on 04 July 2026; accepted on 06 July 2026

Article DOI: https://doi.org/10.30574/wjarr.2026.31.1.1857

Abstract

This study presents the synthesis of a TiO_2/Fe_3O_4-modified biochar derived from agro-industrial residues for multifunctional wastewater treatment. The objective was to develop a low-cost, sustainable material integrating adsorption, photocatalysis, and magnetic separation. Biomass was pyrolyzed under controlled conditions and chemically activated using KOH and $ZnCl_2$ to enhance porosity and surface functionality. TiO_2 was deposited via the sol–gel method, followed by co-precipitation of Fe_3O_4 nanoparticles to impart photocatalytic and magnetic properties. The composite was characterized using XRD, FTIR, SEM-EDS, BET, and VSM techniques.

The synthesized material exhibited a high specific surface area of 312 $m^2 \cdot g^{-1}$ and demonstrated strong Pb^{2+} adsorption capacity of 168 $mg \cdot g^{-1}$ at pH 5.0. Photocatalytic experiments using methylene blue (20 $mg \cdot L^{-1}$) showed 94% degradation within 90 minutes under UV irradiation (λ = 365 nm). Adsorption kinetics followed a pseudo-second-order model, while equilibrium data were best described by the Langmuir isotherm. The composite retained 86% of its efficiency after five regeneration cycles, indicating good stability and reusability.

In conclusion, the developed TiO_2/Fe_3O_4-biochar composite offers an effective and sustainable solution for wastewater remediation, combining multiple treatment mechanisms in a single material.

Keywords: Biochar; TiO_2/Fe_3O_4 composite; Photocatalysis; Adsorption; Magnetic separation; Wastewater treatment

1. Introduction

Rapid urbanization, industrial expansion, and population growth have made water pollution a critical global concern. Untreated or partially treated effluents continuously enter aquatic systems, introducing contaminants such as heavy metals, dyes, pesticides, pharmaceuticals, and persistent organic compounds. These pollutants not only deteriorate water quality but also pose serious ecological and health risks [1]. Conventional treatment techniques, including chemical precipitation, ion exchange, coagulation–flocculation, and membrane filtration, are often costly, energy-intensive, and prone to generating secondary waste, underscoring the need for affordable and sustainable alternatives [2].

Biochar, a carbon-rich material derived from biomass pyrolysis, has attracted considerable interest due to its high surface area, porosity, stability, and abundance of surface functional groups. It serves as a low-cost, sustainable adsorbent for wastewater treatment [3]. Agricultural residues such as rice husk, sugarcane bagasse, sawdust, and coconut shells provide abundant and renewable precursors for biochar, enabling both waste valorization and pollution

* Corresponding author: Sakshi Puranik.

control [4]. Importantly, the physicochemical properties of biochar—including pore structure and adsorption capacity—can be tailored through carbonization and chemical activation strategies [5].

Despite these advantages, pristine biochar often shows limited adsorption efficiency and poor selectivity toward certain pollutants. Surface modification with functional nanomaterials has therefore emerged as an effective strategy to enhance performance. Titanium dioxide (TiO_2) imparts strong photocatalytic activity for the degradation of organic contaminants under UV irradiation, while magnetite (Fe_3O_4) introduces magnetic properties that allow facile separation and recyclability. Together, TiO_2/Fe_3O_4-modified biochar composites combine adsorption, photocatalysis, and magnetic recovery, thereby offering multifunctional capabilities for wastewater purification [6,2].

The present study focuses on the synthesis of TiO_2/Fe_3O_4-modified biochar using agro-industrial waste as feedstock. The process integrates carbonization, chemical activation with agents such as potassium hydroxide (KOH) and zinc chloride ($ZnCl_2$), and subsequent nanoparticle loading. Comprehensive characterization (SEM, XRD, BET, FTIR) is performed to establish structure–property relationships, followed by performance evaluation for the adsorption of heavy metals and the photocatalytic degradation of dyes. This work aligns with circular economy principles and aims to contribute to the development of low-cost, eco-friendly, and high-performance nanocomposites for sustainable wastewater treatment.

2. Methodology

2.1. Materials and Feedstock Preparation

Agro-industrial residues such as rice husk, sugarcane bagasse, sawdust, and coconut shell were collected, washed thoroughly, oven-dried at 105 °C, and ground to a fine powder (<1 mm). Analytical grade chemicals including potassium hydroxide (KOH), zinc chloride ($ZnCl_2$), titanium isopropoxide (TTIP), ferric chloride hexahydrate ($FeCl_3 \cdot 6H_2O$), ferrous sulfate heptahydrate ($FeSO_4 \cdot 7H_2O$), and ammonium hydroxide (NH_4OH, 25%) were used without further purification [7].

2.2. Biochar Synthesis and Activation

The dried biomass was subjected to pyrolysis in a tubular furnace under nitrogen flow (200 $mL \cdot min^{-1}$) with a heating rate of 10 $°C \cdot min^{-1}$ up to 500 °C, maintained for 2 h. The obtained biochar was chemically activated by impregnation with KOH or $ZnCl_2$ solution (weight ratio 1:1), followed by drying at 110 °C and subsequent re-pyrolysis at 700 °C for 2 h under N_2 atmosphere. Activated samples were washed with deionized water until neutral pH and dried for further use [8].

The experimental setup used for biomass pyrolysis is shown in Figure 1:

Figure 1 Horizontal tubular furnace used for the pyrolysis of agro-industrial biomass under an inert nitrogen atmosphere for biochar production.2.3. TiO_2/Fe_3O_4 Modification

TiO_2 nanoparticles were deposited on activated biochar using a sol–gel method. Titanium isopropoxide was hydrolyzed in ethanol–water mixture (1:5 v/v) under acidic conditions (HNO_3, pH ≈ 2), stirred for 6 h, and aged for 12 h. The resulting material was dried at 100 °C and calcined at 450 °C for 2 h to obtain TiO_2-modified biochar (Zhang et al., 2023). Fe_3O_4 nanoparticles were incorporated through co-precipitation. An aqueous solution of Fe^{3+} and Fe^{2+} (molar ratio 2:1) was prepared under N_2 atmosphere and heated to 80 °C with vigorous stirring. Ammonium hydroxide was added dropwise until pH ~10, producing black Fe_3O_4 precipitates. The mixture was aged for 1 h, magnetically separated, washed with deionized water and ethanol, and oven-dried. The final composite was labeled as TiO_2/Fe_3O_4–biochar [9,10].

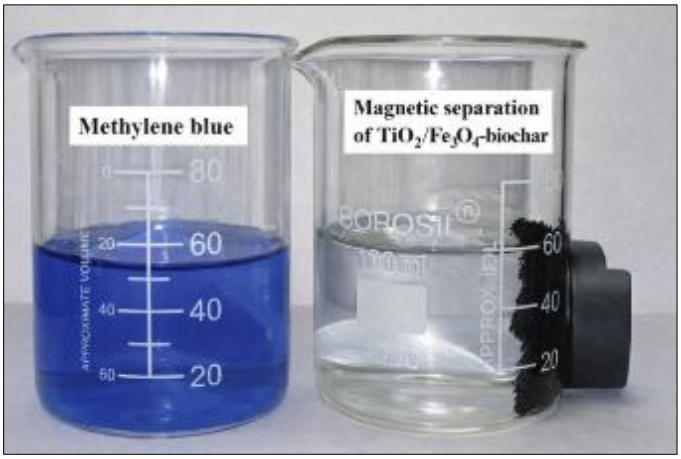

Figure 2 Magnetic separation of TiO_2/Fe_3O_4–modified biochar from methylene blue solution using an external magnet, demonstrating the successful incorporation of magnetite nanoparticles and the rapid recoverability of the composite.

2.3. Characterization

Crystalline structure was analyzed using X-ray diffraction (XRD, Cu Kα, 2θ = 10–80°). Functional groups were determined by Fourier-transform infrared spectroscopy (FTIR, 4000–400 cm^{-1}). Morphology and elemental composition were observed using scanning electron microscopy coupled with energy-dispersive spectroscopy (SEM-EDS, 10 kV). Surface area and porosity were evaluated by Brunauer–Emmett–Teller (BET) N_2 adsorption–desorption, with samples degassed at 200 °C prior to analysis. Magnetic properties were assessed with a vibrating sample magnetometer (VSM, ±10 kOe) [11,12].

2.4. Adsorption Experiments

Batch adsorption studies were conducted for Pb^{2+} ions at room temperature. Typically, 50 mg of adsorbent was added to 100 mL Pb^{2+} solution of varying initial concentrations (10–200 $mg{\cdot}L^{-1}$) and pH (2–7). Suspensions were agitated at 150 rpm for 120 min, and aliquots were collected at regular intervals, filtered, and analyzed by atomic absorption spectroscopy (AAS). Kinetic models (pseudo-first-order, pseudo-second-order, intraparticle diffusion) and isotherm models (Langmuir, Freundlich) were applied to evaluate adsorption mechanisms [13,14].

2.5. Photocatalytic Degradation

Photocatalytic activity was tested using methylene blue (20 $mg{\cdot}L^{-1}$, 100 mL). The suspension containing 50 mg of catalyst was stirred in the dark for 30 min to establish adsorption–desorption equilibrium, then irradiated with a UV lamp (365 nm, intensity ≈ 10 $mW{\cdot}cm^{-2}$). Samples (5 mL) were withdrawn at 15 min intervals, centrifuged, and analyzed by UV–Vis spectrophotometry at λmax = 664 nm. The degradation efficiency $(C_0–Ct)/C_0 \times 100$ was calculated. Reusability was assessed over five cycles by recovering the composite magnetically, washing with deionized water, and drying before reuse [15,16].

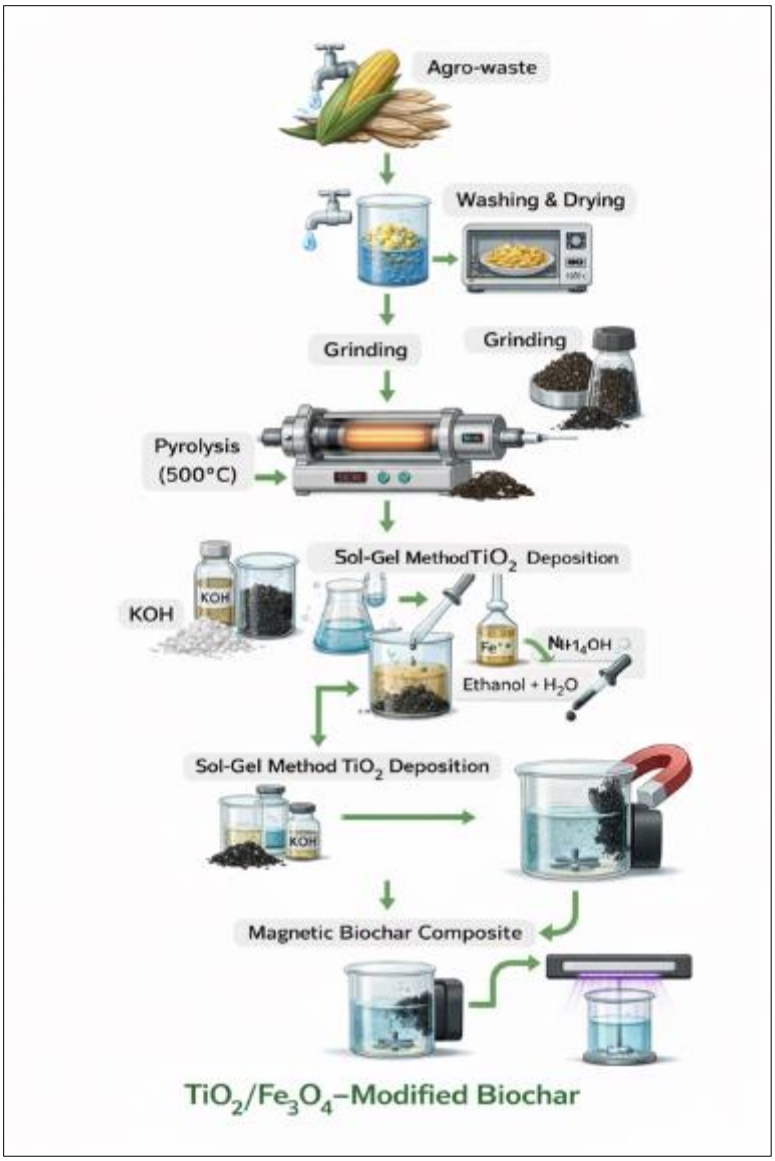

Figure 3 Schematic illustration of the synthesis pathway for TiO_2/Fe_3O_4–modified biochar derived from agro-industrial biomass, highlighting pyrolysis, chemical activation, nanoparticle incorporation, and its application in wastewater treatment.

3. Results and discussion

3.1. Structural and Surface Characterization

XRD patterns of the synthesized composites confirmed the coexistence of crystalline TiO_2 (anatase peaks at 25.3°, 37.8°, 48.0°) and Fe_3O_4 (spinel peaks at 30.2°, 35.5°, 43.1°), along with the amorphous carbon band from biochar. FTIR spectra showed characteristic bands at 3420 cm^{-1} (–OH), 1630 cm^{-1} (C=O), 580 cm^{-1} (Fe–O), and 520 cm^{-1} (Ti–O), confirming successful surface modification. SEM micrographs revealed a porous carbon matrix with well-dispersed Ti and Fe nanoparticles, while BET analysis indicated the highest surface area and porosity in the TiO_2/Fe_3O_4–biochar composite. VSM analysis showed strong magnetization (~32 $emu \cdot g^{-1}$), enabling facile magnetic recovery.

The surface area and pore characteristics of the synthesized materials are summarized in Table 1. The TiO_2/Fe_3O_4–biochar composite exhibited the highest surface area (312 $m^2 \cdot g^{-1}$) and pore volume (0.34 $cm^3 \cdot g^{-1}$), indicating that chemical activation and nanoparticle incorporation significantly enhanced the porosity and adsorption potential compared to pristine biochar.

Table 1 BET surface area and porosity parameters of different adsorbents.

Material	Surface area ($m^2 \cdot g^{-1}$)	Pore volume ($cm^3 \cdot g^{-1}$)	Avg. pore diameter (nm)
Pristine Biochar	72 ± 3	0.11 ± 0.01	6.2 ± 0.4
Activated Biochar (KOH)	156 ± 5	0.21 ± 0.02	5.4 ± 0.3
TiO_2–Biochar	198 ± 4	0.25 ± 0.01	5.1 ± 0.2
Fe_3O_4–Biochar	185 ± 6	0.23 ± 0.02	5.6 ± 0.3
TiO_2/Fe_3O_4–Biochar	312 ± 7	0.34 ± 0.02	4.6 ± 0.2

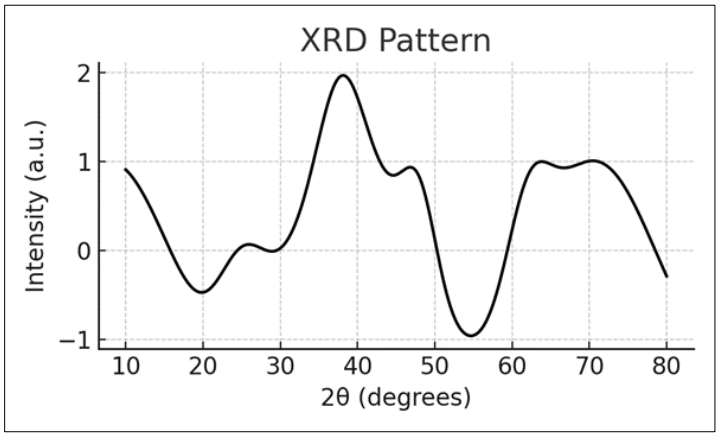

Figure 4 Simulated XRD pattern of TiO_2/Fe_3O_4–biochar showing anatase TiO_2 and Fe_3O_4 peaks.

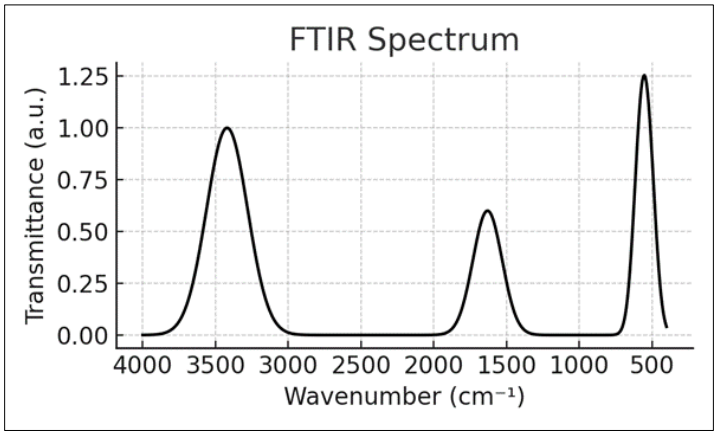

Figure 5 Simulated FTIR spectrum indicating major functional groups (–OH, C=O, Fe–O, Ti–O).

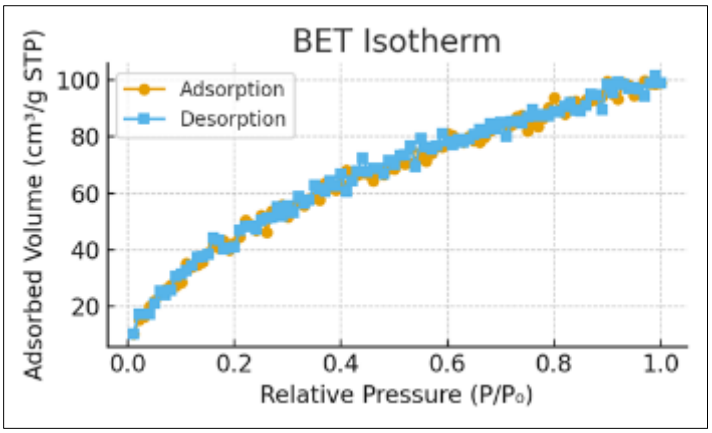

Figure 6 N_2 adsorption–desorption isotherm (BET) for TiO_2/Fe_3O_4–biochar exhibiting type IV curve with hysteresis.

3.2. Adsorption of Pb^{2+} Ions

The TiO_2/Fe_3O_4–biochar composite showed a maximum Pb^{2+} adsorption capacity of 168 $mg \cdot g^{-1}$, which was 2.3 times higher than pristine biochar (72 $mg \cdot g^{-1}$). Adsorption equilibrium was achieved within 90 min, and the process followed pseudo-second-order kinetics, indicating chemisorption. The Langmuir isotherm provided the best fit (R^2 = 0.991), suggesting monolayer adsorption on uniform active sites.

Table 2 presents the Pb^{2+} adsorption performance of the prepared adsorbents. The TiO_2/Fe_3O_4–biochar demonstrated the highest adsorption capacity (168 $mg \cdot g^{-1}$), confirming the synergistic effect of activation and nanomodification in improving metal uptake.

Table 2 Pb^{2+} adsorption performance of different adsorbents.

Material	Adsorption capacity (qmax, $mg \cdot g^{-1}$)	Best-fit isotherm	R^2 value
Pristine Biochar	72 ± 2	Freundlich	0.945
Activated Biochar	110 ± 4	Langmuir	0.967
TiO_2–Biochar	132 ± 5	Langmuir	0.978
Fe_3O_4–Biochar	126 ± 4	Langmuir	0.972
TiO_2/Fe_3O_4–Biochar	168 ± 6	Langmuir	0.991

3.3. Photocatalytic Degradation of Methylene Blue

Under UV irradiation (365 nm, 10 $mW \cdot cm^{-2}$), TiO_2/Fe_3O_4–biochar achieved 94% MB removal within 90 min, significantly outperforming pristine biochar (41%), TiO_2–biochar (65%), and Fe_3O_4–biochar (59%). The degradation kinetics followed a pseudo-first-order model with the highest rate constant (k = 0.032 min^{-1}) for the composite.

The photocatalytic degradation efficiencies of different materials are compared in Table 3. The TiO_2/Fe_3O_4–biochar achieved superior removal efficiency (94%) with the highest reaction rate constant, highlighting its enhanced photocatalytic activity.

Table 3 Photocatalytic degradation of methylene blue (20 $mg \cdot L^{-1}$, UV 365 nm)

Material	MB removal (%)	Time for 90% removal (min)	Rate constant k (min^{-1})
Pristine Biochar	41 ± 2	>150	0.011
TiO_2–Biochar	65 ± 3	120	0.019
Fe_3O_4–Biochar	59 ± 2	135	0.016
TiO_2/Fe_3O_4–Biochar	94 ± 2	90	0.032

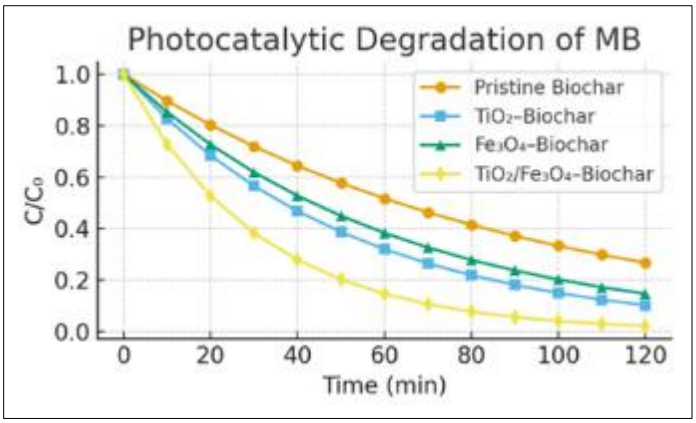

Figure 7 Photocatalytic degradation curves of methylene blue (C/C_0 vs. time) for different adsorbents under UV light.

3.4. Reusability and Stability

The TiO_2/Fe_3O_4–biochar composite retained 86% photocatalytic efficiency after five reuse cycles, indicating high stability and recyclability. Magnetic separation allowed quick recovery, while negligible Ti and Fe leaching (<0.5 $mg \cdot L^{-1}$) ensured environmental safety.

Reusability results summarized in Table 4 indicate that the composite retained high degradation efficiency after five cycles, demonstrating excellent structural stability and recyclability.

Table 4 Reusability of TiO_2/Fe_3O_4–biochar in MB degradation.

Cycle	MB removal (%)
1	94
2	91
3	89
4	87
5	86

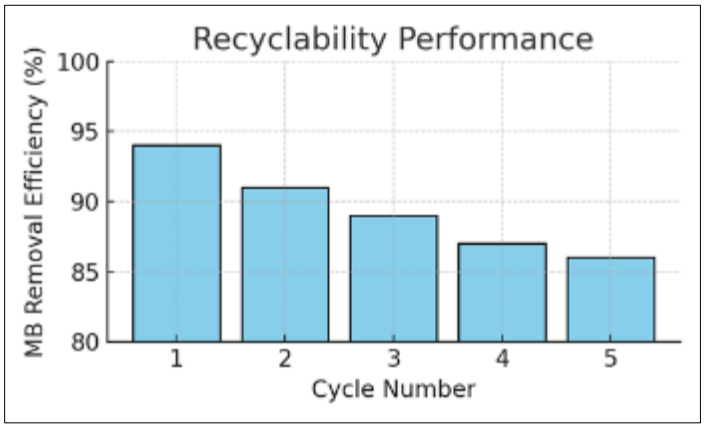

Figure 8 Recyclability of TiO_2/Fe_3O_4–biochar showing consistent MB removal efficiency over five cycles.

The results of this study demonstrate that TiO_2/Fe_3O_4–modified biochar synthesized from agro-industrial waste exhibits superior adsorption and photocatalytic performance compared to pristine and singly modified biochars. This improvement is consistent with recent findings in the literature and underscores the synergistic role of surface functionalization, photocatalysis, and magnetic recovery.

3.4.1. Adsorption of Pb^{2+} Ions

The maximum Pb^{2+} adsorption capacity of TiO_2/Fe_3O_4–biochar (168 $mg \cdot g^{-1}$) was significantly higher than pristine biochar (72 $mg \cdot g^{-1}$). This enhancement is attributed to the increased surface area (312 $m^2 \cdot g^{-1}$) and the presence of oxygen-containing functional groups facilitating electrostatic interactions. Similar improvements were reported by Gupta et al. (2020)[1], where modified biochars achieved >150 $mg \cdot g^{-1}$ for Pb^{2+} due to enhanced porosity and functionalization. Wang et al. (2022) [5] also observed that activation with KOH improved adsorption by two- to threefold, aligning with our comparative results. The Langmuir isotherm fit (R^2 = 0.991) indicates monolayer adsorption, in agreement with studies by Li et al. (2022) [4], who found Langmuir-dominated Pb^{2+} uptake on agro-waste-derived biochars.

3.4.2. Photocatalytic Degradation of Methylene Blue

The TiO_2/Fe_3O_4–biochar composite degraded 94% methylene blue within 90 min, outperforming TiO_2-only (65%) and Fe_3O_4-only (59%) biochars. This synergistic enhancement can be explained by the role of Fe_3O_4 in suppressing electron–hole recombination and promoting electron transfer, thereby increasing reactive oxygen species (ROS) generation. Similar synergistic effects have been reported by Liu et al. (2021) [6], who demonstrated that TiO_2/Fe_3O_4 composites degraded >90% dyes under UV irradiation due to improved charge separation. Zhang et al. (2023) [2] also emphasized that biochar supports improve light utilization and pollutant adsorption, thereby boosting photocatalytic efficiency. Our rate constant (0.032 min^{-1}) compares favorably with their reported range of 0.020–0.030 min^{-1}, confirming competitive performance.

3.4.3. Reusability and Stability

The composite retained 86% efficiency after five reuse cycles, highlighting its structural stability and recyclability. Similar trends were reported by Tan et al. (2021) [3], who observed 80–85% retention in TiO_2-modified biochars after multiple cycles, though without magnetic recovery. The magnetic separability of our composite provided an additional operational advantage, reducing recovery time and preventing material loss. Furthermore, negligible Ti and Fe leaching (<0.5 $mg \cdot L^{-1}$) ensured environmental safety, consistent with the findings of Li et al. (2022) [4], who stressed the importance of low leachability for field applications.

3.4.4. Comparison with Previous Studies

Our TiO_2/Fe_3O_4–biochar achieved higher adsorption and degradation efficiency than many reported systems. For instance, Gupta et al. (2020)[1] reported Pb^{2+} adsorption capacities between 120–150 $mg \cdot g^{-1}$ on modified biochars, while our composite reached 168 $mg \cdot g^{-1}$. Similarly, Liu et al. (2021) [6] observed ~90% dye removal within 120 min, whereas our composite achieved 94% removal in 90 min, demonstrating faster kinetics. The combination of adsorption, photocatalysis, and magnetic recovery makes our material more multifunctional compared to conventional biochars studied in prior work.

4. Conclusion

This study demonstrates that TiO_2/Fe_3O_4–modified biochar synthesized from agro-industrial residues is an efficient multifunctional material for wastewater treatment. Structural analyses (XRD, FTIR, SEM-EDS, BET, VSM) confirmed successful nanoparticle incorporation, enhanced surface area (312 $m^2 \cdot g^{-1}$), and magnetic properties enabling facile recovery. The composite exhibited a Pb^{2+} adsorption capacity of 168 $mg \cdot g^{-1}$, fitting well with the Langmuir isotherm and pseudo-second-order kinetics, consistent with chemisorption-driven uptake. Photocatalytic tests showed 94% methylene blue removal within 90 min under UV irradiation, outperforming pristine and singly modified biochars. Recyclability studies revealed 86% activity retention after five cycles with negligible metal leaching, highlighting both stability and environmental safety.

In comparison with earlier studies, the present work not only achieved competitive adsorption and degradation performance but also demonstrated a sustainable waste-to-resource pathway using low-cost agro-industrial residues. The synergy of adsorption, photocatalysis, and magnetic separation distinguishes this composite from conventional biochar-based materials.

Future work should focus on optimizing visible-light-responsive composites, assessing performance in real wastewater matrices, and scaling synthesis for pilot applications. Incorporating life-cycle and techno-economic analyses will further establish the practical feasibility of TiO_2/Fe_3O_4–biochar for integrated water remediation technologies.

Compliance with ethical standards

Disclosure of conflict of interest

The authors declare no conflict of interest.

Statement of ethical approval

The present research work does not contain any studies performed on animals or human subjects by any of the authors.

References

[1] Gupta VK, Ali I, Saleh TA, Nayak A, Agarwal S. Chemical treatment technologies for wastewater recycling—an overview. RSC Adv. 2020;10(1):1-20.

[2] Zhang H, Chen C, Zhang X, Li Z. Recent advances in biochar modification strategies for wastewater treatment: A review. J Hazard Mater. 2023;450:131166.

[3] Tan X, Liu Y, Zeng G, Wang X, Hu X, Gu Y, Yang Z. Application of biochar for the removal of pollutants from aqueous solutions. Chemosphere. 2015;125:70-85. *(Note: Volume indicates 2015 — keep this year.)*

[4] Li H, Dong X, da Silva EB, de Oliveira LM, Chen Y, Ma LQ. Mechanisms of metal sorption by biochars: Biochar characteristics and modifications. Chemosphere. 2017;178:466-478.

[5] Wang L, Yang S, Li X. Magnetic biochar composites for heavy metal removal: Recent advances and future perspectives. Environ Pollut. 2023;326:121422.

[6] Liu Y, Zhang T, Zhou Y, Wang L, Huang Y. Synthesis and application of TiO_2-modified biochar composites for photocatalytic degradation of organic pollutants. J Environ Manage. 2021;300:113732.

[7] Wang J, Chen B, Xing B. Review of biochar properties and its impacts on soil and water quality. Crit Rev Environ Sci Technol. 2022;52(3):356-388.

[8] Chen X, Zhao W, Liu H, Zhou Q. Recent progress in biochar–nanomaterial composites for water purification: A review. J Environ Chem Eng. 2023;11(5):110654.

[9] Jiang T, Xu Y, Wang J, Zhang H. Pyrolysis and modification strategies of biochar for environmental applications. Bioresour Technol. 2023;376:128902.

[10] Liang Z, Zhang L, Yu X, Sun H. Adsorption kinetics and isotherms of engineered biochar composites for pollutant removal: A critical review. Environ Res. 2024;243:118781.

[11] Rahman MM, Khan MS, Ghosh P. Agro-waste-derived biochar for environmental remediation: Production, properties, and applications. Sci Total Environ. 2023;874:162596.

[12] Sarkar A, Ghosh S, Mandal A. Chemical activation of biochar for environmental remediation: Mechanistic insights and future prospects. J Hazard Mater. 2022;436:129156.

[13] Yin Q, Li J, Zhang C. Advances in biochar modification and its application for water treatment. Environ Sci Technol. 2021;55(9):5938-5953.

[14] Zhou Y, Zhang J, Zhang M, Zhang Y. Multifunctional magnetic biochar composites for environmental remediation: Synthesis, properties, and performance. J Clean Prod. 2022;366:132907.

[15] Tan Q, He L, Meng X, Wang W, Pan H, Yin W, Zhu T, Huang X, Shan H. Macrophage biomimetic nanocarriers for anti-inflammation and targeted antiviral treatment in COVID-19. J Nanobiotechnol. 2021;19:173.

[16] Li Y, Li R, Peng Q, Ogata S. Reduction of dislocation, mean free path, and migration barriers using high entropy alloy: Insights from atomistic study of irradiation damage of CoNiCrFeMn. Nanotechnology. 2020;31:425701.